

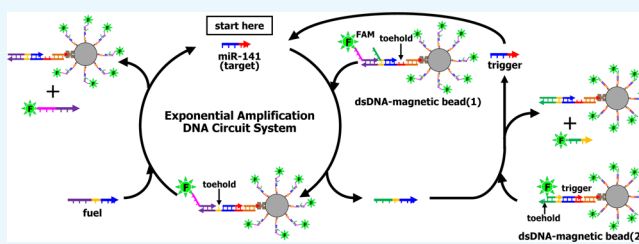
Comparative Study of DNA Circuit System-Based Proportional and Exponential Amplification Strategies for Enzyme-Free and Rapid Detection of miRNA at Room Temperature

Motoi Oishi*

Division of Materials Science, Faculty of Pure and Applied Sciences, University of Tsukuba, 1-1-1 Tennoudai, Tsukuba, Ibaraki 305-8573, Japan

Supporting Information

ABSTRACT: Because circulating microRNAs (miRNAs) have been recognized as a new class of blood-based biomarkers for various diseases, a significant challenge has been the development of point-of-care testing (POCT) systems based on detection of circulating miRNAs directly from serum. A promising approach to POCT systems is considered to be the development of enzyme-free and isothermal detection systems. Here, two types of DNA circuit system based on proportional and exponential amplification strategies were constructed using double-stranded DNA-modified magnetic beads (dsDNA-MBs) and their performances for detection of miRNA were studied comparatively. Both proportional and exponential amplification DNA circuit systems enabled the detection of target miRNA (miR-141) at room temperature without the need for additional enzymes because miR-141 acted as a catalyst for successive toehold-mediated DNA displacement reactions. A significant increase in the noise fluorescence signal was observed for the exponential amplification DNA circuit system because of the leakage (undesired DNA displacement reaction) revealed by the kinetic study on each DNA displacement reaction. Nevertheless, the exponential amplification DNA circuit system showed a lower limit of detection (LOD: 46 pM) and shorter assay time (15 min) compared to those of the proportional amplification DNA circuit system (LOD: 103 pM at 180 min). It is most likely that the exponential amplification DNA circuit system enabled amplification of both the signals and target miR-141, whereas the proportional amplification DNA circuit system enabled amplification of the signals alone. In addition, the exponential amplification DNA circuit system was able to discriminate between mismatched base sequences in miR-200 family members and specifically detect miR-141 even in the presence of serum. These findings are important for the rational design for POCT systems.



INTRODUCTION

Circulating microRNAs (miRNAs) have been recognized as a new class of relatively noninvasive (i.e., blood-based) biomarkers for various diseases because expression profiles of miRNAs are reported to be different between abnormal and normal cells.^{1–4} A significant challenge is to detect circulating miRNAs directly from serum because of their possible application to point-of-care testing (POCT) systems.^{5–7} Currently, the quantitative reverse transcription polymerase chain reaction (qRT-PCR) method is the “gold standard method” for expression profiling analysis of circulating miRNA in serum samples.^{8–10} However, coexisting materials in serum easily inhibit enzymatic reactions, including synthesis of complementary DNA (cDNA) through reverse transcription of miRNA and amplification of cDNA based on PCR. Therefore, miRNA-specific qRT-PCR still requires tedious processes such as the isolation of total miRNA from exosomes in serum samples.^{11–14} Additional problems for miRNA-specific qRT-PCR are the use of instruments to precisely control thermal cycling. On the basis of these facts, miRNA-specific qRT-PCR is considerably difficult to use for POCT systems. Hence, a promising approach to POCT systems is believed to be the

development of an enzyme-free and isothermal assay system, achieving detection of miRNAs directly from serum samples.

A new class of enzyme-free and isothermal system, entropy-driven catalytic reaction (the so-called DNA circuit system),¹⁵ has been devised on the basis of successive toehold-mediated DNA displacement reactions.¹⁶ The DNA circuit system enables to amplify signals proportionally at room temperature without any enzymes or instruments because the target DNA (RNA) catalyzes successive toehold-mediated DNA displacement reactions.^{17–21} Although proportional amplification DNA circuit systems have been used for the detection of miRNAs, an assay time over several hours is needed to detect low concentrations of target miRNAs. Meanwhile, DNA circuit systems based on an exponential amplification strategy have also been reported,^{15,22,23} which enable amplification of both signals and target nucleic acids, and thus, PCR-like, this system is considered to be the best candidate for miRNA-based POCT systems. However, the number of reports on exponential amplification DNA circuit

Received: November 28, 2017

Accepted: February 14, 2018

Published: March 20, 2018

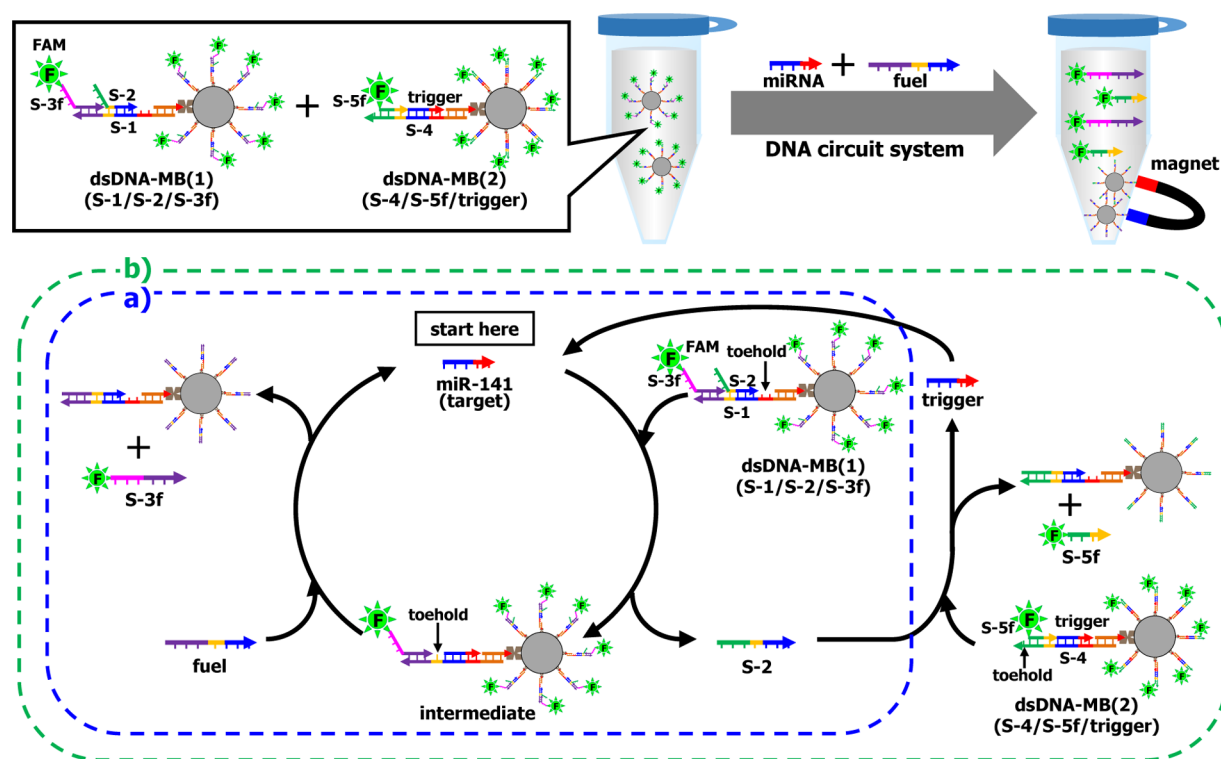


Figure 1. Schematic illustration of the principles of DNA circuit systems based on (a) proportional and (b) exponential amplification strategies.

systems is limited and furthermore comparative studies of the analytical performances of proportional and exponential amplification DNA circuit systems have not been reported. Accordingly, it is important to clarify the performance and problems of the exponential amplification DNA circuit system when considering the rational design for POCT systems.

As presented here, two types of a DNA circuit system based on proportional (Figure 1a) and exponential amplification strategies (Figure 1b) were constructed using double-stranded DNA-modified magnetic beads (dsDNA-MBs) and their analytical performances, including the limit of detection (LOD), assay time, and kinetics were studied comparatively. One of the most troublesome defects in DNA circuit systems is leakage, causing the generation of noise signals even in the absence of the target nucleic acid, caused by (i) impurity of dsDNAs and (ii) undesired DNA displacement reactions.¹⁵ Because the source of dsDNA impurity (single-stranded DNAs) is mainly partially formed dsDNA due to imperfect stoichiometry, dsDNA should be purified by electrophoresis to ensure proper stoichiometry and improve purity. The use of dsDNA-MB in place of free dsDNA does not require the time-consuming purification of dsDNA by electrophoresis because impurity of dsDNA-MB is easily removed by washing under a magnetic field, eliminating the leakage by dsDNA impurity. Both proportional and exponential amplification DNA circuit systems were able to detect target miRNA at room temperature without any enzymes. Unlike the proportional amplification DNA circuit system, a significant increase in the noise signal was observed for the exponential amplification DNA circuit system due to the leakage caused by undesired DNA displacement reactions. Nevertheless, the exponential amplification DNA circuit system showed lower LOD and shorter assay time compared to that of the proportional amplification DNA circuit system. Eventually, the exponential amplification DNA circuit system allows for a rapid assay for

detecting target miRNA at concentrations as low as 46 pM in 15 min, as well as discriminating base-mismatched miR-200 family sequences.

RESULTS AND DISCUSSION

Design Principle of Proportional and Exponential Amplification DNA Circuits. The current study reports on a comparative study of the proportional and exponential amplification strategies for DNA circuit systems (Figure 1). Table S1 shows miRNA and DNA sequences used in this study. As a proof of concept, hsa-miR-141 (miR-141) was chosen as a target miRNA because expression profiles of miR-141 in serum are reported to be different between healthy persons and cancer patients.²⁴ Two types of dsDNA (1) (S-1/S-2/S-3f) and dsDNA (2) (S-4/S-5f/trigger) were added to DNA-modified MB to prepare dsDNA-MBs (1) (S-1/S-2/S-3f) and (2) (S-4/S-5f/trigger), respectively, and the resulting dsDNA-MBs (1) (S-1/S-2/S-3f) and (2) (S-4/S-5f/trigger) were washed repeatedly with buffer under a magnetic field to remove any impurity (undesired single-stranded DNAs). The target miR-141 causes the toehold-mediated DNA displacement reaction with DNA (S-2) in dsDNA-MB (1) (S-1/S-2/S-3f), resulting in the formation of an intermediate containing a newly formed toehold structure. Subsequently, the release of the miR-141 and a 6-carboxy-fluorescein (FAM)-labeled DNA (S-3f) from the intermediate occurs by fuel DNA through the toehold-mediated DNA displacement reaction. The released target miR-141 can be recycled as a catalyst for the DNA circuit, and the proportional amplification of the fluorescence signal starts a new (proportional amplification strategy: Figure 1a). Additionally, the released DNA (S-2) induces the release of trigger DNA and FAM-labeled DNA (S-5f) from dsDNA-MB (2) (S-4/S-5f/trigger) through the toehold-mediated DNA displacement reaction. The released trigger DNA can also act as a catalyst

for the DNA circuit because of the sequence of trigger DNA being identical to that of the miR-141, and the exponential amplification of both the fluorescence signal and the trigger DNAs equivalent with miR-141 occurs (exponential amplification strategy: Figure 1b). Thus, the exponential amplification DNA circuit system is a simple expansion of the proportional amplification DNA circuit system, allowing an easy comparison of their analytical performances.

Performance of Proportional and Exponential Amplification DNA Circuits. To evaluate the proportional amplification DNA circuit, dsDNA-MB (1) (S-1/S-2/S-3f) ($[\text{dsDNA (1) (S-1/S-2/S-3f)}] = 10 \text{ nM}$) was incubated in 10 mM Tris-HCl buffer pH 7.7 containing 12.5 mM MgCl₂, 150 mM NaCl, and 0.01 (v/v %) Tween 20 in the presence of fuel DNA (10 nM) and various concentrations of miR-141 (100 pM to 8 nM). Fluorescence intensity in the mixture was monitored at 522 nm at 25 °C for 180 min; the fluorescence intensity was normalized as follows: normalized $F = (F_t - F_0)/(F_{\text{max}} - F_0)$, where F_t , F_{max} , and F_0 are fluorescence intensities at t min, 10 nM of dsDNA (1) (S-1/S-2/S-3f), and 0 min, respectively. Notably, a significant increase in the normalized F was observed for the mixture of dsDNA-MB (1) (S-1/S-2/S-3f), fuel DNA, and miR-141 with different concentrations (Figure 2) and both the values

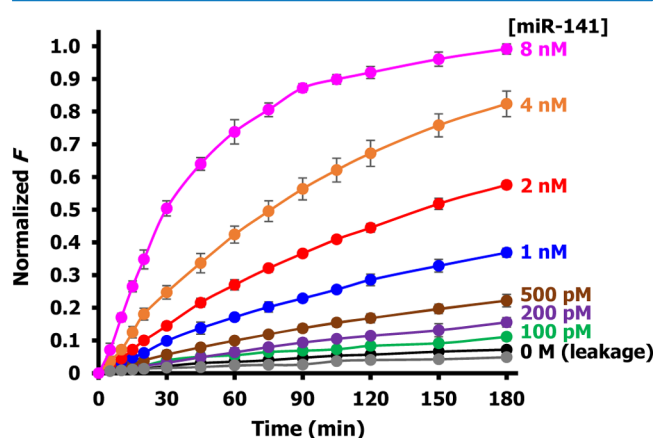


Figure 2. Normalized F of the proportional DNA circuit system as a function of time at different miR-141 concentrations in the presence of fuel DNA (10 nM). Normalized F represents that 1.0 is the fluorescence of 10 nM of FAM. Gray circles are normalized F of the dsDNA-MB (1) (S-1/S-2/S-3f) alone. Mean values and standard deviations were obtained from three independent experiments.

and increase rates of the normalized F are concentration-dependent on miR-141. However, the mixture of dsDNA-MB (1) (S-1/S-2/S-3f) and fuel DNA showed a slight increase in the normalized F even in the absence of miR-141 due to leakage caused by an undesired entropy-driven DNA displacement reaction between fuel DNA and dsDNA-MB (1) (S-1/S-2/S-3f). Consequently, 100 pM of miR-141 could be detectable within 180 min and the turnover number of miR-141 is roughly four cycles (100 pM of miR-141 reacted with 397 pM of dsDNA (1) (S-1/S-2/S-3f) on dsDNA-MB (1) (S-1/S-2/S-3f) above the baseline set by the presence of fuel DNA and absence of miR-141). These facts obviously demonstrate that proportional amplification of the normalized F is due to a miR-141-triggered DNA circuit mechanism.

An exponential amplification DNA circuit system was constructed by adding dsDNA-MB (2) (S-4/S-5f/trigger) to a mixture containing the dsDNA-MB (1) (S-1/S-2/S-3f), fuel

DNA, and miR-141. Ideally, this DNA circuit system should enable amplification of both the normalized F as well as the trigger DNA (equivalent to miR-141) by 2^n -fold, with n being the number of circuit cycles. Figure 3a shows the normalized F as a function of time at different concentrations of miR-141 (10 pM to 5 nM). The normalized F exhibited a typical sigmoidal curve with an abrupt increase and a plateau after 180 min. In addition, the normalized F in the absence of miR-141 showed a substantial increase after 30 min. Note that the time needed to reach the normalized F of 0.4 (the C_t value) was also proportionally dependent on the log-concentration of miR-141 at 50 pM to 5 nM (Figure 3b), strongly indicating exponential amplification of both the fluorescence signal and the trigger DNA (miR-141). Taken together, these findings revealed that the concentration of miR-141 was responsible for the rise time of the normalized F . The delayed exponential increase in the normalized F observed even in the absence of miR-141 is most likely due to the released DNA (S-2) by leakage through an undesired DNA displacement reaction between fuel DNA and dsDNA-MB (1) (S-1/S-2/S-3f), viz., the released DNA (S-2) starts nonspecific amplification of both the fluorescence signal and the trigger DNA.

Kinetic Study on the Proportional and Exponential Amplification DNA Circuits. The toehold-mediated DNA displacement reaction involves a two-step process. The first step is to form several base pairs at the toeholds, and then the second step is a branch migration process to form complete dsDNA along with the release of outgoing DNA. A model of bimolecular kinetic can be applied to the kinetics of the toehold-mediated DNA displacement reactions.^{25–27} Figure 4 shows models of each toehold-mediated DNA displacement reaction in both proportional and exponential amplification DNA circuit systems. Because the toehold-mediated DNA displacement reactions with an appropriate toehold length proceed rapidly, the back reactions can be negligible (see the Supporting Information).²⁵ To estimate the individual rate constants k_1 , k_2 , k_3 , k_4 , k_5 , k_{L1} , and k_{L2} , all DNA displacement reactions were carried out in 10 mM Tris-HCl buffer pH 7.7 containing 150 mM NaCl, 12.5 mM MgCl₂, and 0.01 (v/v %) Tween 20 at 25 °C, with all DNA concentrations of 10 nM. The time-dependent increase in the fluorescence signal in the mixture was monitored (Figure S1), and the rate constants were determined from the equation (see eq SI4 in the Supporting Information). Note that the rate constants k_1 ($4.2 \times 10^5 \text{ M}^{-1} \text{ s}^{-1}$), k_2 ($1.3 \times 10^5 \text{ M}^{-1} \text{ s}^{-1}$), k_4 ($6.0 \times 10^5 \text{ M}^{-1} \text{ s}^{-1}$), and k_5 ($3.4 \times 10^5 \text{ M}^{-1} \text{ s}^{-1}$) are of the same order of magnitude as the rate constants of the DNA circuit system using free DNA in solution.¹⁵ Additionally, the rate constant k_3 ($3.7 \times 10^4 \text{ M}^{-1} \text{ s}^{-1}$) was the lowest among k_1 – k_5 , indicating that this process is the rate-determining step in both proportional and exponential amplification DNA circuit systems. The lower rate constant observed for k_3 is presumably due to a shorter toehold length (4 nt) compared to that of other toehold-mediated DNA displacement reactions (6 nt). However, significantly lower rate constants k_{L1} ($5.5 \times 10^2 \text{ M}^{-1} \text{ s}^{-1}$) and k_{L2} ($9.0 \times 10 \text{ M}^{-1} \text{ s}^{-1}$) were observed for leakage caused by entropy-driven DNA displacement reactions between fuel DNA and dsDNA-MB (1) (S-1/S-2/S-3f) and rate constant k_{L1} was one-order higher than k_{L2} . Therefore, the proportional amplification DNA circuit system can amplify signal generation by over 2 orders of magnitude ($k_3/k_{L2} = 411$). Meanwhile, the nonspecific amplification observed for the exponential amplification DNA circuit system (Figure 3) is due to the low k_3/k_{L1} ratio ($= 67$), viz., the released DNA (S-2) by leakage causes the release of trigger DNA from dsDNA-MB (2) (S-4/S-5f/trigger).

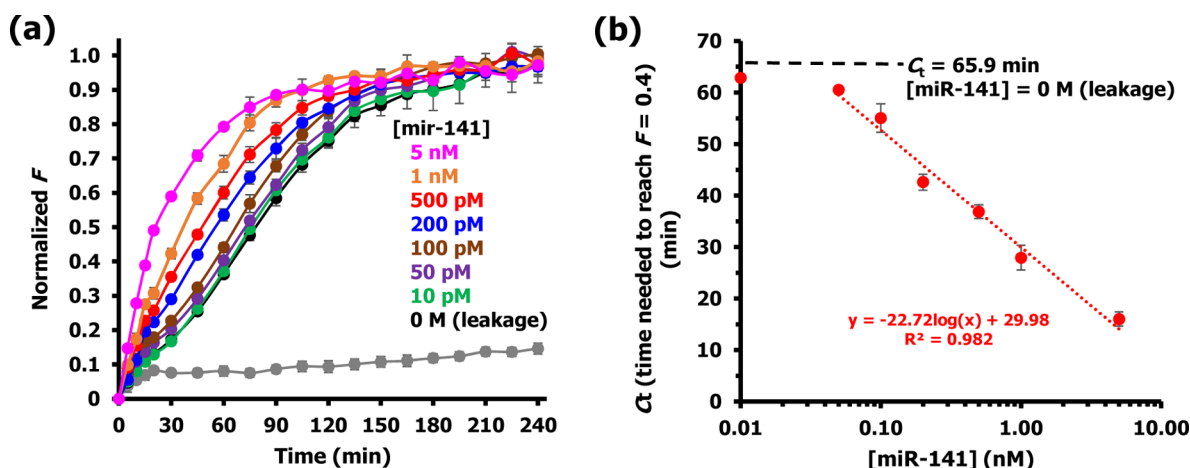


Figure 3. (a) Normalized F of the exponential DNA circuit system as a function of time at different miR-141 concentrations in the presence of fuel DNA (10 nM). Normalized F represents that 1.0 is the fluorescence of 20 nM FAM. Gray circles are normalized F of the mixture of dsDNA-MB (1) (S-1/S-2/S-3f) and dsDNA-MB (2) (S-4/S-5f/trigger) in the absence of fuel DNA. (b) The corresponding calibration curve of miR-141 concentration vs C_t (time needed to reach the normalized F of 0.4) for the exponential DNA circuit system. Mean values and standard deviations were obtained from three independent experiments.

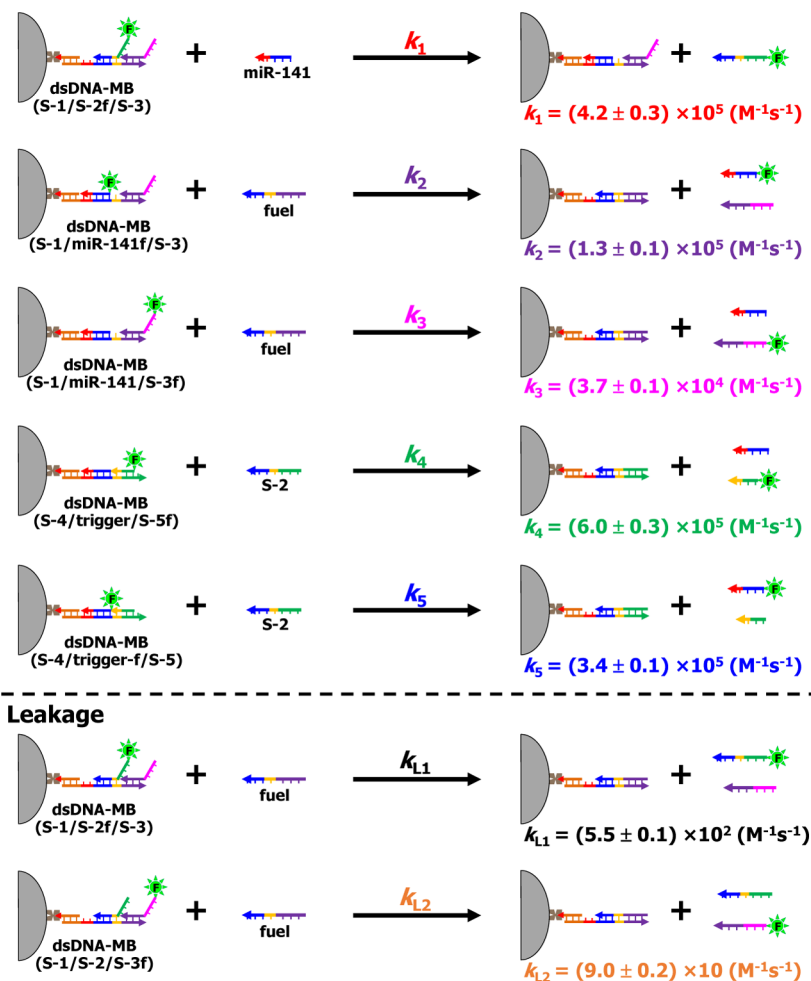


Figure 4. Kinetic models of the proportional and exponential DNA circuit systems and the rate constant values of each DNA displacement reaction. Mean values and standard deviations were obtained from three independent experiments.

Sensitivity and Assay Times of Proportional and Exponential Amplification DNA Circuits. Figure 5 shows the normalized F of both proportional (Figure 5a) and exponential amplification DNA circuit systems (Figure 5b)

with various concentrations of miR-141 at different assay times (15, 30, 45, 60, 120, and 180 min). The normalized F of proportional and exponential amplification DNA circuit systems proportionally correlated to the concentration of miR-141, and

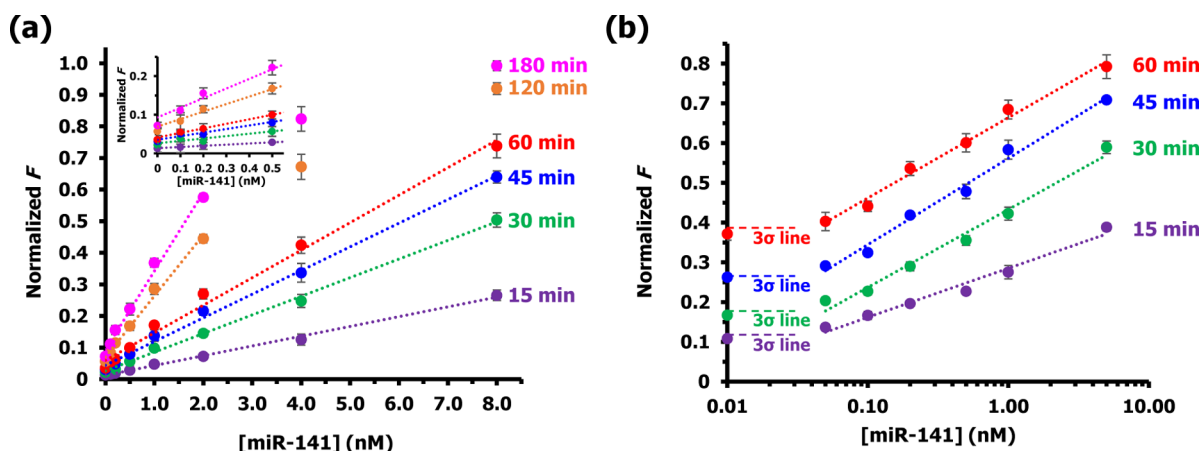


Figure 5. (a) Normalized F of the proportional DNA circuit system with various concentrations of miR-141 at different assay times (15 min: $y = 0.030x + 0.011$, $R^2 = 0.98$, 30 min: $y = 0.058x + 0.023$, $R^2 = 0.99$, 45 min: $y = 0.074x + 0.040$, $R^2 = 0.99$, 60 min: $y = 0.087x + 0.048$, $R^2 = 0.99$, 120 min: $y = 0.192x + 0.065$, $R^2 = 0.99$, and 180 min: $y = 0.246x + 0.088$, $R^2 = 0.99$). Normalized F represents that 1.0 is the fluorescence of 10 nM of FAM. The inset shows the responses to 0–1.0 nM of miR-141. (b) Normalized F of the exponential DNA circuit system with various concentrations of miR-141 at different assay times (15 min: $y = 0.123 \log(x) + 0.285$, $R^2 = 0.98$, 30 min: $y = 0.196 \log(x) + 0.433$, $R^2 = 0.98$, 45 min: $y = 0.217 \log(x) + 0.562$, $R^2 = 0.99$, and 60 min: $y = 0.202 \log(x) + 0.664$, $R^2 = 0.99$). Normalized F represents that 1.0 is the fluorescence of 20 nM of FAM. 3σ lines represent values of normalized F at 0 M (leak signal) + 3σ at different assay times. Mean values and standard deviations were obtained from three independent experiments using different diluent stock solutions.

Table 1. LODs at Different Assay Times (15, 30, 45, 60, 120, and 180 min) of the Proportional And Exponential DNA Circuit Systems^a

	15 min	30 min	45 min	60 min	120 min	180 min
LODs of proportional DNA circuit system ^b	1.1 nM	279 pM	240 pM	192 pM	119 pM	103 pM
LODs of exponential DNA circuit system ^b	46 pM	50 pM	42 pM	42 pM		

^aMean values and standard deviations were obtained from three independent experiments using different diluent stock solutions. ^bCalculated 3 times the standard deviation (σ) of the leak signal, i.e., normalized F at 0 M (leak signal) + 3σ .

the LODs (calculated 3 times the standard deviation (σ) of the leak signal, i.e., normalized F at 0 M (leak signal) + 3σ) are summarized in Table 1. The LODs of the proportional amplification DNA circuit system decreased with an increase in assay time, achieving the lowest LOD (103 pM) after 180 min. This is due to proportional amplification of normalized F caused by the miR-141-triggered DNA circuit mechanism. In sharp contrast, the LODs of the exponential amplification DNA circuit system did not depend on assay time (15–60 min), viz., LODs were found to be almost constant values (40–50 pM) due to nonspecific exponential amplification caused by leakage. It should be noted that the LODs of the exponential amplification DNA circuit system had an LOD (46 pM) even after 15 min that was ca. 20-fold lower compared to that of the proportional amplification DNA circuit system (LOD: 1.1 nM at 15 min). Because the concentration of miR-141 was responsible for the rise time of the normalized F , the real-time fluorescence signal curves could be used as the measure for quantitative analysis of miR-141. The LOD was also calculated to be 36 pM from Figure 3b. Moreover, the exponential amplification DNA circuit system had a dynamic range over 3 orders of magnitude of miR-141 concentrations and the dynamic range of the exponential amplification DNA circuit system was wider than that of the proportional amplification DNA circuit system. The lower LOD, shorter assay time, and wider dynamic range are based on the exponential amplification of both the normalized F and the trigger DNA.

Specificity of Exponential Amplification DNA Circuit. Another important consideration is specificity because miRNA family members are known to have homologous sequences.

Target miR-141 belongs to miR-200 family members, including miR-429, miR-200a, miR-200b, and miR-200c.²⁴ A similar assay procedure was employed for the exponential amplification DNA circuit system using miR-200 family members. Figure 6 shows the comparison between the normalized F at 15 min of different miRNAs (100 pM and 1 nM), and Figure S2 also shows the normalized F as a function of time and C_i values. Note that

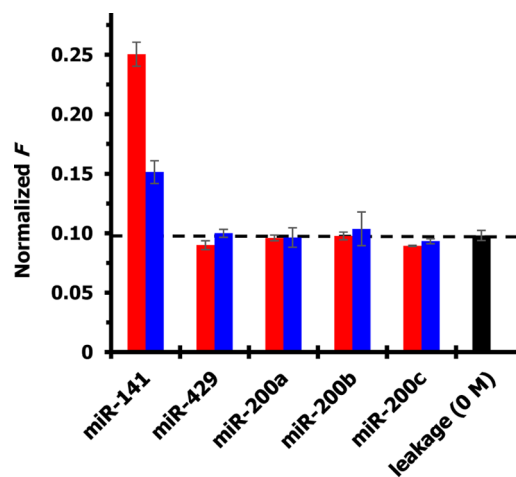


Figure 6. Normalized F of the exponential DNA circuit system when analyzing 1 nM (red bars) and 100 pM (blue bars) of miR-141 (target miRNA) and mismatch miRNAs (miR-429, miR-200a, miR-200b, and miR-200c). Mean values and standard deviations were obtained from three independent experiments.

normalized F at 15 min and C_t values of miR-200 family members except for miR-141 were similar to those of the leakage (miRNA = 0 M) and miR-141 induced the highest normalized F and the smallest C_t values, demonstrating that the exponential amplification DNA circuit system allows for discriminating between other miR-200 family members and miR-141. These results are due to the high capability of toehold-mediated DNA displacement reactions to discriminate mismatched base sequences.²⁸

Detection of Target miRNA in the Presence of Serum by Exponential Amplification DNA Circuit. To demonstrate the feasibility of a more practical application of the exponential amplification DNA circuit system, detection of miR-141 from exosome-free fetal bovine serum (Exo-FBS) was conducted by spiking different concentrations of miR-141 (100 pM and 1 nM) into Exo-FBS. Exo-FBS as a realistically complex matrix is known to inhibit enzymatic reactions used in qRT-PCR.^{11–14} Table 2

Table 2. Detection of miR-141 in the Absence or Presence of FBS (10%) by the Exponential DNA Circuit System

miR-141	FBS (-)		10% FBS (+)		recovery (%)
	normalized F^a C_t (min) ^a	RSD (%)	normalized F^a C_t (min) ^a	RSD (%)	
100 pM	0.17 ± 0.01	6.1	0.16 ± 0.01	6.2	95.3
	55.0 ± 1.6	2.8	56.9 ± 1.9	3.3	103.3
1 nM	0.28 ± 0.02	6.1	0.26 ± 0.01	5.6	95.5
	27.9 ± 1.4	5.0	29.0 ± 1.4	4.9	103.9

^aMean values and standard deviations were obtained from three independent experiments.

shows the normalized F at 15 min and C_t values at different concentrations of miR-141 (100 pM and 1 nM) in the presence (10%) and absence of FBS, and Figure S3 also shows the normalized F as a function of time. Notably, the exponential amplification DNA circuit system showed no change in normalized F at 15 min or C_t values with high reproducibility, even in the presence of 10% FBS. Thus, satisfactory recovery (95.3–103.9%) and a low relative standard deviation (RSD: 2.8–6.2%) were observed, indicating serum does not interfere with the exponential amplification DNA circuit process through successive toehold-mediated DNA displacement reactions. These results indicate that the exponential amplification DNA circuit system shows great promise as a practical application for the detection of miRNAs directly from real samples.

CONCLUSIONS

The current study describes a comparative study of DNA circuit system-based proportional and exponential amplification strategies for enzyme-free detection of miRNA at room temperature. The proportional and exponential amplification DNA circuit systems were constructed using dsDNA-MBs. The use of dsDNA-MBs in place of free dsDNAs allowed easy elimination of the leakage caused by impurity of dsDNA because impurity of dsDNA-MBs is easily removable by washing under a magnetic field without the time-consuming purification process by electrophoresis. Both proportional and exponential amplification DNA circuit systems were able to detect miR-141 at room temperature without the need for additional enzymes because the miR-141 acted as a catalyst for successive toehold-mediated DNA displacement reactions. A slight increase in noise fluorescence signal was observed for the proportional amplification DNA circuit system, whereas the exponential

amplification DNA circuit system showed a significant increase in noise fluorescence signal due to the leakage caused by undesired DNA displacement reactions. The kinetic study of each toehold DNA displacement reaction in DNA circuit systems revealed that ratio (k_3/k_{L1}) of rate constants of the rate-determining step (k_3) and leakage step (k_{L1}) for the exponential amplification DNA circuit system was lower than that for the proportional amplification DNA circuit system (k_3/k_{L2}), indicating that this finding was in accordance with the observed noise signals. Nevertheless, the exponential amplification DNA circuit system showed a lower LOD (46 pM) and shorter assay time (15 min) compared with those of the proportional amplification DNA circuit system (LOD: 103 pM in 180 min). In addition, the exponential amplification DNA circuit system was able to discriminate between differences in base mismatches in miR-200 family members and detect miR-141 even in the presence of serum. These findings revealed that suppression of the leakage in the exponential amplification DNA circuit system is an important issue for the development of miRNA-based POCT systems.

EXPERIMENTAL SECTION

Chemicals and Instruments. Trizma-pH 7.7 (Sigma-Aldrich), Tween 20 (Wako, Japan), magnesium chloride hexahydrate (MgCl₂: Wako, Japan), sodium chloride (NaCl: Wako, Japan), 3 μm of MagnoshereM300/streptavidin (MB: JSR Life Sciences, Japan), guanidine thiocyanate (Wako, Japan), and exosome-depleted fetal bovine serum medium (FBS: System Biosciences, Inc.) were used without further purification. Water was purified using the Milli-Q system (Millipore). Oligonucleotides (DNAs and RNAs) were purchased from Japan Bio Service, Co., Japan, and the DNA and RNA sequences employed are shown in Table S1. Fluorescence spectra were recorded using a Quantus fluorometer (Promega). All incubation processes were performed with a Thermo shaker incubator (ALLSHENG, China).

Preparation of dsDNA (1) (S-1/S-2/S-3f) and (2) (S-4/S-5f/Trigger). For preparation of dsDNA (1), 10 mM Tris-HCl buffer solutions at pH 7.7 with 150 mM NaCl and 0.01 (v/v %) Tween 20 of S-1 (20 μM, 20 μL), S-2 (40 μM, 20 μL), and S-3f (40 μM, 20 μL), and 10 mM Tris-HCl buffer pH 7.7 containing 150 mM NaCl and 0.01 (v/v %) Tween 20 (300 μL) were mixed. For preparation of dsDNA (2), 10 mM Tris-HCl buffer solutions at pH 7.7 with 150 mM NaCl and 0.01 (v/v %) Tween 20 of S-4 (20 μM, 20 μL), trigger (20 μM, 40 μL), and S-5f (20 μM, 40 μL), and 20 mM Tris-HCl buffer (300 μL) were mixed. The resulting mixtures were annealed at 95 °C for 5 min and allowed to cool to room temperature over the course of 120 min. Each final concentration of dsDNAs (1) and (2) was 1 μM with excess single-stranded DNAs (S-2, S-3f, trigger, and S-5f).

Preparation of dsDNA-MB (1) (S-1/S-2/S-3f) and (2) (S-4/S-5f/Trigger). To prepare the DNA-MB, streptavidin-modified MB (1000 μL, 10 mg mL⁻¹, 6 × 10⁸ MBs mL⁻¹) was washed three times using 10 mM Tris-HCl buffer pH 7.7 containing 150 mM NaCl and 0.01 (v/v %) Tween 20 (1000 μL). A solution of biotin-labeled capture DNA in 10 mM Tris-HCl buffer pH 7.7 with 150 mM NaCl and 0.01 (v/v %) Tween 20 (20 μM, 400 μL) was added to MB, and the mixture was incubated with gentle mixing at 25 °C for 60 min. The DNA-MB was pulled to the wall of the reaction tube by application of a magnetic field. The DNA-MB was then washed three times using 10 mM Tris-HCl buffer pH 7.7 containing 150 mM NaCl and 0.01 (v/v %) Tween 20 (1000 μL). The DNA-MB was dispersed in 10 mM Tris-HCl buffer pH 7.7 containing 150 mM NaCl and

0.01 (v/v %) Tween 20 to adjust 6×10^8 MBs mL⁻¹ concentration. To quantify the amount of immobilized capture DNA strands on MB, FAM-labeled capture DNA (capture DNA-F) was used in place of capture DNA. Procedures for the preparation and the purification of FAM-labeled capture DNA-modified MB were the same as those described above. Fluorescence intensity at 522 nm aliquots of the supernatant were converted to molar concentrations of capture DNA-F by interpolation from a standard linear calibration curve prepared with known concentrations of capture DNA-F using identical buffer pH, salt, and Tween 20 concentrations. The average number of capture DNA-F per MB particle was $(2.16 \pm 0.17) \times 10^6$ strands per MB (immobilization efficiency: 27%), calculated by dividing the measured DNA molar concentration by the MB concentration.

A solution of DNA-MB in 10 mM Tris-HCl buffer pH 7.7 containing 150 mM NaCl and 0.01 (v/v %) Tween 20 (200 μ L, 1.2×10^8 MBs) was added to a 1.5 mL PCR tube, and the DNA-MB was pulled to the wall of the reaction tube by application of a magnetic field to remove buffer solution. Each solution of dsDNAs (1) and (2) in 10 mM Tris-HCl buffer pH 7.7 containing 150 mM NaCl and 0.01 (v/v %) Tween 20 (76 μ L, [dsDNA (1)] = [dsDNA (2)] = 1 μ M) was separately added to DNA-MB (1.2×10^8 MBs) to prepare dsDNA-MB (1) and dsDNA-MB (2), respectively, and the mixtures were incubated with gentle mixing at 25 °C for 60 min. The dsDNA-MB (1) and dsDNA-MB (2) were pulled to the wall of the reaction tube by application of a magnetic field. Both dsDNA-MB (1) and dsDNA-MB (2) were then washed three times using 10 mM Tris-HCl buffer pH 7.7 containing 150 mM NaCl and 0.01 (v/v %) Tween 20 (400 μ L), and supernatants were corrected to quantify the amount of immobilized dsDNA (1) and (2) strands on MB. In addition, fresh 10 mM Tris-HCl buffer pH 7.7 containing 150 mM NaCl and 0.01 (v/v %) Tween 20 (1000 μ L) was added to the dsDNA-MB (1) and dsDNA-MB (2) and the mixtures were incubated further with gentle mixing at 25 °C for 6 h to remove nonspecific adsorbed dsDNAs (1) and (2). The dsDNA-MB (1) and dsDNA-MB (2) were pulled to the wall of the reaction tube by application of a magnetic field and washed three times using 10 mM Tris-HCl buffer pH 7.7 containing 150 mM NaCl and 0.01 (v/v %) Tween 20 (400 μ L). Fluorescence intensity at 522 nm of all supernatants was converted to molar concentrations of dsDNAs (1) and (2) by interpolation from a standard linear calibration curve prepared with known concentrations of dsDNAs (1) and (2) using identical buffer pH, salt, and Tween 20 concentrations. The average number of dsDNAs (1) and (2) per dsDNA-MB (1) and dsDNA-MB (2) was $(2.70 \pm 0.21) \times 10^5$ strands per MB (immobilization efficiency: 71%) and $(2.82 \pm 0.15) \times 10^5$ strands per MB (immobilization efficiency: 74%), respectively, as calculated by dividing the measured DNA molar concentration by the MB concentration. The dsDNA-MB (1) and dsDNA-MB (2) were dispersed in 10 mM Tris-HCl buffer pH 7.7 containing 150 mM NaCl and 0.01 (v/v %) Tween 20 to adjust 50 nM concentrations of dsDNAs (1) and (2).

Detection of miR-141 by the Proportional Amplification DNA Circuit System. A solution of the dsDNA-MB (1) in 10 mM Tris-HCl buffer pH 7.7 containing 150 mM NaCl and 0.01 (v/v %) Tween 20 (40 μ L, [dsDNA (1)] = 50 nM) was added to a 0.5 mL PCR tube, and the dsDNA-MB (1) was pulled to the wall of the reaction tube by application of a magnetic field to remove buffer solution. To the dsDNA-MB (1), 10 mM Tris-HCl buffer pH 7.7 containing 150 mM NaCl and 0.01 (v/v %)

Tween 20 (170 μ L), 10 mM Tris-HCl buffer pH 7.7 containing 150 mM NaCl, 0.01 (v/v %) Tween 20, and 250 mM of MgCl₂ (10 μ L), fuel DNA in 10 mM Tris-HCl buffer pH 7.7 containing 150 mM NaCl and 0.01 (v/v %) Tween 20 (200 nM, 10 μ L), and various concentrations of miR-141 solutions in 10 mM Tris-HCl buffer pH 7.7 containing 150 mM NaCl and 0.01 (v/v %) Tween 20 (2–160 nM, 10 μ L) were added, and the total volume was 200 μ L. Final concentrations of Mg²⁺, dsDNA (1), fuel DNA, and miR-141 were 12.5 mM, 10 nM, 10 nM, and 100 pM to 8 nM, respectively. The resulting mixture was incubated with gentle mixing at 25 °C for 180 min. During the incubation, fluorescence intensity at 522 nm was measured at appropriate time intervals after precipitation of dsDNA-MB (1) by application of a magnetic field. Furthermore, measured fluorescence intensity was normalized as follows $(F_t - F_0)/(F_{\max} - F_0)$, where F_t , F_{\max} and F_0 are fluorescence intensity at t min, fluorescence intensity at 10 nM of dsDNA (1), and fluorescence intensity at 0 min, respectively.

Detection of miR-141 by the Exponential Amplification DNA Circuit System. A solution of the dsDNA-MB (1) in 10 mM Tris-HCl buffer pH 7.7 containing 150 mM NaCl and 0.01 (v/v %) Tween 20 (40 μ L, [dsDNA (1)] = 50 nM) was added to a 0.5 mL PCR tube, and the dsDNA-MB (1) was pulled to the wall of the reaction tube by application of a magnetic field to remove buffer solution. To the dsDNA-MB (1), a solution of the dsDNA-MB (2) in 10 mM Tris-HCl buffer pH 7.7 containing 150 mM NaCl and 0.01 (v/v %) Tween 20 (40 μ L, [dsDNA (2)] = 50 nM) was added, and both the dsDNA-MB (1) and dsDNA-MB (2) were pulled to the wall of the reaction tube by application of a magnetic field to remove buffer solution. To the mixture of dsDNA-MB (1) and dsDNA-MB (2), 10 mM Tris-HCl buffer pH 7.7 containing 150 mM NaCl and 0.01 (v/v %) Tween 20 (170 μ L), 10 mM Tris-HCl buffer pH 7.7 containing 150 mM NaCl, 0.01 (v/v %) Tween 20, and 250 mM of MgCl₂ (10 μ L), fuel DNA in 10 mM Tris-HCl buffer pH 7.7 containing 150 mM NaCl and 0.01 (v/v %) Tween 20 (200 nM, 10 μ L), and various concentrations of miR-141 solutions in 10 mM Tris-HCl buffer pH 7.7 containing 150 mM NaCl and 0.01 (v/v %) Tween 20 (20 pM to 100 nM, 10 μ L) were added, and the total volume was 200 μ L. Final concentrations of Mg²⁺, dsDNA (1), fuel DNA, and miR-141 were 12.5 mM, 10 nM, 10 nM, and 1 pM to 5 nM, respectively. The resulting mixture was incubated with gentle mixing at 25 °C for 180 min. During the incubation, fluorescence intensity at 522 nm was measured at appropriate time intervals after precipitation of the dsDNA-MB (1) and the dsDNA-MB (2) by application of a magnetic field. Furthermore, the measured fluorescence intensity was normalized as follows: $(F_t - F_0)/(F_{\max} - F_0)$, where F_t , F_{\max} and F_0 are fluorescence intensity at t min, total fluorescence intensity at 10 nM of dsDNA (1) and at 10 nM of dsDNA (2), and fluorescence intensity at 0 min, respectively.

Determination of Rate Constants of DNA Displacement Reactions. To determine the individual rate constants k_1 , k_2 , k_3 , k_4 , k_5 , k_{L1} , and k_{L2} , FAM-labeled DNAs (S-2f and trigger-f) and FAM-miR-141 (miR-141f) were also used. The procedures for the preparation and the purification of dsDNA-MBs were identical to those described above. Each DNA displacement reaction was carried out in 10 mM Tris-HCl buffer pH 7.7 containing 150 mM NaCl, 0.01 (v/v %) Tween 20, and 12.5 mM of MgCl₂ at 25 °C, and final concentrations of dsDNAs and other single-stranded DNAs and RNAs (fuel DNA, S-2, miR-141, and miR-141f) were same as 10 nM. During the incubation, fluorescence intensity at 522 nm was measured at appropriate

time intervals after precipitation of the dsDNA-MBs by application of a magnetic field. Furthermore, measured fluorescence intensity was normalized as follows: $(F_t - F_{\text{blank}})/(F_{\text{max}} - F_{\text{blank}})$, where F_t , F_{max} , and F_{blank} are fluorescence intensity at t s, fluorescence intensity at 10 nM of dsDNA, and fluorescence intensity of dsDNA-MB alone at t s, respectively. Thus, normalized F corresponds to the reaction efficiency (0–1) of each DNA displacement reaction. Figure S1a,b shows the time-dependent increase in normalized F , and the rate constants k_1 , k_2 , k_3 , k_4 , k_5 , k_{L1} , and k_{L2} were determined from the fitting eq S14 (see the Supporting Information) using normalized F values and the kinetic model (see the Supporting Information).

Discrimination of Base Mismatches in miR-141 Family Members. Except for the use of miR-429, miR-200a, miR-200b, and miR-200c (100 pM and 1 nM), the detection procedure and conditions were identical to those described above.

Detection of miR-141 in the Presence of Serum. A solution of guanidine thiocyanate in 10 mM Tris–HCl buffer pH 7.7 containing 150 mM NaCl and 0.01 (v/v %) Tween 20 (4 M, 500 μ L) was added to exosome-free FBS (500 μ L) to deactivate DNase and RNase, and the FBS–guanidine mixture was incubated for 10 min at room temperature. Solutions of miR-141 in 10 mM Tris–HCl buffer pH 7.7 containing 150 mM NaCl and 0.01 (v/v %) Tween 20 (95.4 nM and 0.954 nM, 10 μ L) were separately added to the FBS–guanidine mixture (190 μ L), and the total volume of FBS solutions was 200 μ L ([FBS] = 49.7% (v/v), [guanidine thiocyanate] = 1.9 M, [miR-141] = 4.77 and 0.477 nM). The resulting FBS (42 μ L) solutions containing miR-141 (4.77 and 0.477 nM) were used to the assay mixture, as described above. Final concentrations of FBS, guanidine thiocyanate, and miR-141 were 10%, 0.4 M, and 1.0 nM or 100 pM, respectively, and the detection procedure and conditions were identical to those described above. Although increase in fluorescence intensity was observed for all samples containing FBS, the normalized F values were the same as those of the samples in the absence of FBS.

■ ASSOCIATED CONTENT

● Supporting Information

The Supporting Information is available free of charge on the ACS Publications website at DOI: 10.1021/acsomega.7b01866.

DNA and RNA sequences, kinetic model for toehold-mediated DNA displacement reaction, rate constant values, normalized F as a function of the time using mismatch miRNAs, and normalized F as a function of the time in the presence of FBS (PDF)

■ AUTHOR INFORMATION

Corresponding Author

*E-mail: oishi@ims.tsukuba.ac.jp. Phone/Fax: +81-29-853-5935.

ORCID

Motoi Oishi: 0000-0002-1032-2164

Notes

The author declares no competing financial interest.

■ ACKNOWLEDGMENTS

This work was partially supported by a Grant-in-Aid for Scientific Research (C) (No. 15K04632) from the Japan Society for the Promotion of Science (JSPS), Translational Research Network Program Seed (A) from Japan Agency for Medical Research and

Development (AMED), and the research grant from The Towa Foundation for Food Science & Research.

■ REFERENCES

- (1) Heneghan, H. M.; Miller, N.; Lowery, A. J.; Sweeney, K. J.; Newell, J.; Kerin, M. J. Circulating microRNAs as novel minimally invasive biomarkers for breast cancer. *Ann. Surg.* **2010**, *251*, 499–505.
- (2) Kosaka, N.; Iguchi, H.; Ochiya, T. Circulating microRNA in body fluid: A new potential biomarker for cancer diagnosis and prognosis. *Cancer Sci.* **2010**, *101*, 2087–2092.
- (3) Turchinovich, A.; Weiz, L.; Langheinz, A.; Burwinkel, B. Characterization of extracellular circulating microRNA. *Nucleic Acids Res.* **2011**, *39*, 7223–7233.
- (4) Arroyo, J. D.; Chevillet, J. R.; Kroh, E. M.; Ruf, I. K.; Pritchard, C. C.; Gibson, D. F.; Mitchell, P. S.; Bennett, C. F.; Pogosova-Agadjanyan, E. L.; Stirewalt, D. L.; Tait, J. F.; Tewari, M. Argonaute2 complexes carry a population of circulating microRNAs independent of vesicles in human plasma. *Proc. Natl. Acad. Sci. U.S.A.* **2011**, *108*, 5003–5008.
- (5) Hartman, M. R.; Ruiz, R. C. H.; Hamada, S.; Xu, C.; Yancey, K. G.; Yu, Y.; Hane, W.; Luo, D. Point-of-care nucleic acid detection using nanotechnology. *Nanoscale* **2013**, *5*, 10141–10154.
- (6) Vaca, L. Point-of-care diagnostic tools to detect circulating microRNAs as biomarkers of disease. *Sensors* **2014**, *14*, 9117–9131.
- (7) Lewis, J. M.; Heineck, D. P.; Heller, M. J. Detecting cancer biomarkers in blood: Challenges for new molecular diagnostic and point-of-care tests using cell-free nucleic acids. *Expert Rev. Mol. Diagn.* **2015**, *15*, 1187–1200.
- (8) Chen, C.; Ridzon, D. A.; Broomer, A. J.; Zhou, Z.; Lee, D. H.; Nguyen, J. T.; Barbisin, M.; Xu, N. L.; Mahuvakar, V. R.; Andersen, M. R.; Lao, K. Q.; Livak, K. J.; Guegler, K. J. Real-time quantification of microRNAs by stem-loop RT-PCR. *Nucleic Acids Res.* **2005**, *33*, No. e179.
- (9) Ro, S.; Park, C.; Jin, J.; Sanders, K. M.; Yan, W. A. A PCR-based method for detection and quantification of small RNAs. *Biochem. Biophys. Res. Commun.* **2006**, *351*, 756–763.
- (10) Fiedler, S. D.; Carletti, M. Z.; Christenson, L. K. Quantitative RT-PCR methods for mature microRNA expression analysis. *Methods Mol. Biol.* **2010**, *630*, 49–64.
- (11) Konet, D. S.; Mezencio, J. M. S.; Babcock, G.; Brown, F. J. Inhibitors of RT-PCR in serum. *J. Virol. Methods* **2000**, *84*, 95–98.
- (12) Al-Soud, W. A.; Rådström, P. Effects of Amplification facilitators on diagnostic PCR in the presence of blood, feces, and meat. *J. Clin. Microbiol.* **2000**, *38*, 4463–4470.
- (13) Kermekchiev, M. B.; Kirilova, L. I.; Vail, E. E.; Barnes, W. M. Mutants of TaqDNA polymerase resistant to PCR inhibitors allow DNA amplification from whole blood and crude soil samples. *Nucleic Acids Res.* **2009**, *37*, No. e40.
- (14) Schrader, C.; Schielke, A.; Ellerbroek, L.; Johne, R. PCR inhibitors—occurrence, properties and removal. *J. Appl. Microbiol.* **2012**, *113*, 1014–1026.
- (15) Zhang, D. Y.; Turberfield, A. J.; Yurke, B.; Winfree, E. Engineering entropy-driven reactions and networks catalyzed by DNA. *Science* **2007**, *318*, 1121–1125.
- (16) Yurke, B.; Turberfield, A. J.; Mills, A. P., Jr.; Simmel, F. C.; Neumann, J. L. A DNA-fueled molecular machine made of DNA. *Nature* **2000**, *406*, 605–608.
- (17) Shi, K.; Dou, B.; Yang, C.; Chai, Y.; Yuan, R.; Xiang, Y. DNA-fueled molecular machine enables enzyme-free target recycling amplification for electronic detection of microRNA from cancer cells with highly minimized background noise. *Anal. Chem.* **2015**, *87*, 8578–8583.
- (18) Li, X.; Li, D.; Zhou, W.; Chai, Y.; Yuan, R.; Xiang, Y. A microRNA-activated molecular machine for non-enzymatic target recycling amplification detection of microRNA from cancer cells. *Chem. Commun.* **2015**, *51*, 11084–11087.
- (19) Shi, K.; Dou, B.; Yang, J.; Yuan, R.; Xiang, Y. Cascaded strand displacement for non-enzymatic target recycling amplification and label-free electronic detection of microRNA from tumor cells. *Anal. Chim. Acta* **2016**, *916*, 1–7.

(20) Oishi, M.; Sugiyama, S. An efficient particle-based DNA circuit system: Catalytic disassembly of DNA/PEG-modified gold nanoparticle-magnetic bead composites for colorimetric detection of miRNA. *Small* **2016**, *12*, 5153–5158.

(21) Liao, Y.; Huang, R.; Ma, Z.; Wu, Y.; Zhou, X.; Xing, D. Target-triggered enzyme-free amplification strategy for sensitive detection of microRNA in tumor cells and tissues. *Anal. Chem.* **2014**, *86*, 4596–4604.

(22) Bi, S.; Zhang, J.; Hao, S.; Ding, C.; Zhang, S. Exponential amplification for chemiluminescence resonance energy transfer detection of microRNA in real samples based on a cross-catalyst strand-displacement network. *Anal. Chem.* **2011**, *83*, 3696–3702.

(23) Bi, S.; Zhang, J.; Hao, S.; Ding, C.; Zhang, S. Correction to exponential amplification for chemiluminescence resonance energy transfer detection of microRNA in real samples based on a cross-catalyst strand-displacement network. *Anal. Chem.* **2011**, *83*, 4326.

(24) Mitchell, P. S.; Parkin, R. K.; Kroh, E. M.; Fritz, B. R.; Wyman, S. K.; Pogosova-Agadjanyan, E. L.; Peterson, A.; Noteboom, J.; O'Brian, K. C.; Allen, A.; Lin, D. W.; Urban, N.; Drescher, C. W.; Knudsen, B. S.; Stirewalt, D. L.; Gentleman, R.; Vessella, R. L.; Nelson, P. S.; Martin, D. B.; Tewari, M. Circulating microRNAs as stable blood-based markers for cancer detection. *Proc. Natl. Acad. Sci. U.S.A.* **2008**, *105*, 10513–10518.

(25) Yurke, B.; Mills, A. P., Jr. Using DNA to power nanostructures. *Genet. Program. Evol. Mach.* **2003**, *4*, 111–122.

(26) Zhang, D. Y.; Winfree, E. Control of DNA strand displacement kinetics using toehold exchange. *J. Am. Chem. Soc.* **2009**, *131*, 17303–17314.

(27) Srinivas, N.; Ouldrige, T. E.; Sulc, P.; Schaeffer, J. M.; Yurke, B.; Louis, A. A.; Doye, J. P. K.; Winfree, E. On the biophysics and kinetics of toehold-mediated DNA strand displacement. *Nucleic Acids Res.* **2013**, *41*, 10641–10658.

(28) Chen, S. X.; Seelig, G. An engineered kinetic amplification mechanism for single nucleotide variant discrimination by DNA hybridization probes. *J. Am. Chem. Soc.* **2016**, *138*, 5076–086.